

## LITERATURE CITED

1. E. H. Cheng and M. N. Ozisik, Intern. J. Heat Mass Transfer, 25, No. 3 (1972).
2. W. G. England and A. F. Emery, Trans. ASME, Ser. C: J. Heat Transfer, 91, No. 1 (1969).
3. R. Cess, in: Advances in Heat Transfer, Vol. 1, Academic Press, New York (1963), pp. 1-50.
4. E. M. Sparrow and J. L. Gregg, Trans. ASME, Ser. C: J. Heat Transfer, 78, 435 (1956).
5. A. V. Furman and A. S. Nenishev, Izv. Akad. Nauk SSSR, Énerg. Transport, No. 3, 104 (1973).
6. V. V. Salomatov and E. M. Puzyrev, Inzh.-Fiz. Zh., 20, No. 6 (1968).
7. V. V. Salomatov and E. M. Puzyrev, in: Modern Problems of Thermal Gravitational Convection [in Russian], Nauka i Tekhnika, Minsk (1968).
8. S. K. Godunov and V. S. Ryaben'kii, Difference Schemes [in Russian], Nauka, Moscow (1973).
9. I. S. Berezin and I. P. Zhidkov, Computing Methods [in Russian], Vol. 2, Fizmatgiz, Moscow (1959).

### NUMERICAL ANALYSIS OF SUPERSONIC FLOW OF AN IDEAL GAS IN THE WAKE OF AN AXISYMMETRICAL BODY

V. V. Bulanov

UDC 518:517.944/947

A numerical experiment is carried out on supersonic flow in the wake of an axisymmetrical body, and estimates are obtained for the "scheme" (artificial) viscosity introduced by a maximally stable difference scheme [1] into the investigated flow.

#### 1. Statement of the Problem

Many papers have been published in the period from 1965 through 1975 on the numerical solution of problems involving the flow of a viscous liquid and a compressible gas in the wake of a body with separation points and reverse-circulation flow zones. In the majority of those papers the complete system of Navier — Stokes equations is approximated by a finite-difference scheme of first or second order, which is then solved by some suitable numerical or iterative technique.

However, solutions of the complete system of Navier — Stokes equations are obtained only for relatively small to moderate (values of a few hundred) Reynolds numbers (see, e.g., [3,4]). The numerical results obtained in these studies mainly corroborate the schematic representations of the flow pattern both in the separation zone and in the wake as a whole.

Very few results have been published on the numerical study of supersonic flows in the wakes of bodies at high and very high Reynolds numbers.

A modern approach that offers fuller understanding and investigation of the singular characteristics of flow at large Reynolds numbers is the application of shock-smearing (or shock-capturing) finite-difference schemes, which approximate the system of Euler equations rather than the complete system of Navier — Stokes equations (see, e.g., [5,6]).

The numerical solutions generated by such investigations may be viewed as numerical experiments, which correspond in their principal features to the true flow pattern for sufficiently large Reynolds numbers and yet are useful not only for the deeper insight that they offer into the singular flow characteristics at corners, in aft and wake zones, etc., but also for exhibiting the capabilities and singular characteristics of the difference scheme itself, for example the influence of the spatial mesh size of the computing grid, type of artificial viscosity, etc., on the accuracy of computation.

---

Translated from Inzhenerno-Fizicheskii Zhurnal, Vol. 32, No. 6, pp. 1080-1086, June, 1977. Original article submitted March 25, 1976.

*This material is protected by copyright registered in the name of Plenum Publishing Corporation, 227 West 17th Street, New York, N.Y. 10011. No part of this publication may be reproduced, stored in a retrieval system, or transmitted, in any form or by any means, electronic, mechanical, photocopying, microfilming, recording or otherwise, without written permission of the publisher. A copy of this article is available from the publisher for \$7.50.*

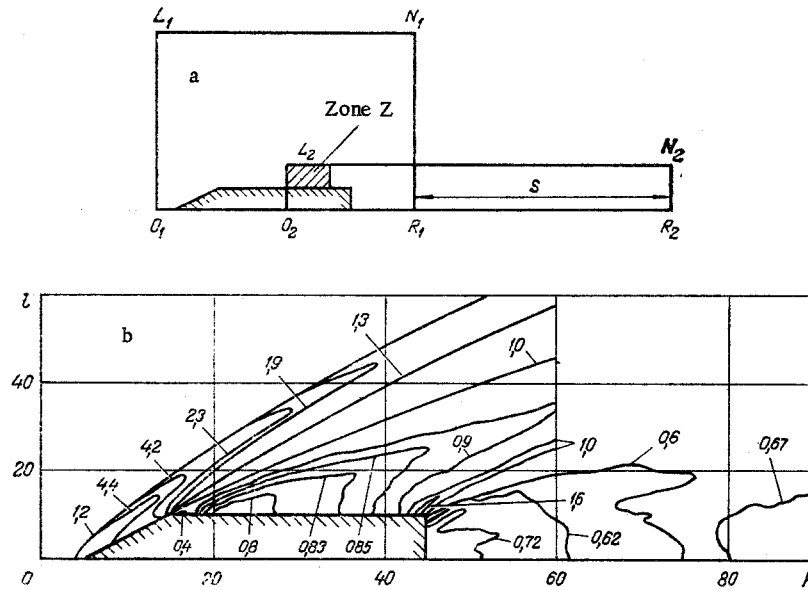


Fig. 1. Field of isobars obtained by matching of the pressure fields in the two stages. a) Computing regions by stages; b) pressure field for  $M_\infty = 2.84$ .

We touch on some of these problems in the present article, which is concerned with the numerical solution of the problem of supersonic ideal-gas flow past an axisymmetrical body of cone – cylinder configuration at freestream Mach number 2.84. The half-angle of the conical part of the body is  $30^\circ$ , and the ratio of the length of the cylindrical part of the body to its diameter is 2.5.

The problem is solved in two stages: 1) At the initial time the field of parameters corresponding to instantaneous plunging of the body into a supersonic flow is specified; 2) then the process of transition to a steady distribution of parameters comprising a solution of the flow problem is analyzed. The flow parameters in the first stage are calculated in the region  $O_1L_1N_1R_1$  (see Fig. 1a), which has dimensions of  $60 \times 100$  mesh units. The flow parameters in the second stage are calculated in the region  $O_2L_2N_2R_2$ , which has different dimensions from those of the region  $O_1L_1N_1R_1$ , comprising  $20 \times 300$  (or  $40 \times 150$ ) mesh units. As the initial data we adopt the first-stage solution, which is obtained by relaxation. For the initial flow parameters we use their values in the zone A adjacent to the lateral surface of the cylindrical part of the body.

## 2. Results of the Computations

The mathematical model of nonsteady axisymmetrical flow is the system of Euler equations with appropriate initial and boundary conditions. The system of equations is written in divergence form:

$$\frac{\partial f}{\partial t} + \frac{\partial}{\partial x} F(f) + \frac{\partial}{\partial y} G(f) + \frac{\nu}{y} H(f) = 0 \quad (1)$$

using the vector notation

$$f = \begin{pmatrix} \rho \\ \rho u \\ \rho v \\ e \end{pmatrix}, \quad F = \begin{pmatrix} \rho u \\ \rho u^2 + p \\ \rho uv \\ (e + p)u \end{pmatrix}, \quad G = \begin{pmatrix} \rho v \\ \rho uv \\ \rho v^2 + p \\ (e + p)v \end{pmatrix}, \quad H = \begin{pmatrix} \rho v \\ \rho uv \\ \rho v^2 \\ (e + p)v \end{pmatrix}.$$

The parameter  $\nu$  characterizes the type of symmetry:  $\nu = 1$  for the axisymmetrical, and  $\nu = 0$  for the planar case.

Together with the general system (1), for uncoupling of the two-dimensional difference operator into one-dimensional operators we introduce the auxiliary one-dimensional systems

$$\frac{\partial \bar{f}}{\partial t} + \frac{\partial}{\partial x} F(\bar{f}) = 0, \quad (2)$$

$$\frac{\partial \bar{f}}{\partial t} + \frac{\partial}{\partial y} G(\bar{f}) + \frac{\nu}{y} H(\bar{f}) = 0. \quad (3)$$

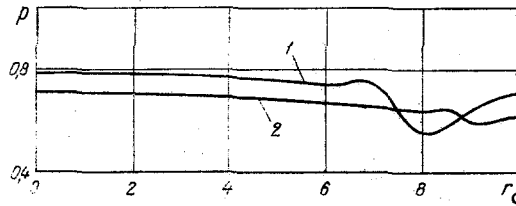


Fig. 2. Radial variation of aft pressure.  
1)  $\Delta y = 0.05$ ,  $\Delta x = 0.1$ ; 2)  $\Delta y = 0.025$ ,  $\Delta x = 0.05$ .

The differencing approximation of the system is made on the grid

$$x_k = k\Delta x, k = 0, 1, 2, \dots; y_l = l\Delta y, l = 0, 1, 2, \dots; t^n = \sum_{i=0}^n \Delta t^i$$

with constant mesh spacings for the spatial coordinates and time spacings determined from the stability condition, which may be written in the form

$$\alpha = \frac{\Delta t^n}{\Delta x} (|u| + \bar{a})^n \leq 1, \lambda = \frac{\Delta t^n}{\Delta y} (|v| + \bar{a})^n \leq 1. \quad (4)$$

To approximate the system of equations (1) on the basis of expressions (2) and (3) we use a maximally stable explicit artificial-viscosity second-order difference scheme, which is described in detail in [1]. We therefore omit the description of the scheme itself and merely indicate the artificial-viscosity expressions:

$$B^n = \delta x Q_{k,l}^n + \delta y R_{k,l}^n, \quad (5)$$

in which

$$Q_{k+\frac{1}{2},l}^n = \frac{\omega}{2} |\delta x \alpha_{k+\frac{1}{2},l}^n| \delta x f_{k+\frac{1}{2},l}^n, R_{k,l+\frac{1}{2}}^n = \frac{\omega}{2} |\delta y \lambda_{k,l+\frac{1}{2}}^n| \delta y f_{k,l+\frac{1}{2}}^n,$$

$\delta$  is the difference operator, and  $\omega$  is a coefficient that varies between 1.0 and 1.5.

The computations are carried out in dimensionless parameters, to which the problem is reduced with the freestream pressure and density and the radius of the cylindrical part of the body adopted as independent characteristic scale units.

In the first stage the computing grid has 6000 mesh points, including 60 with respect to  $x$  and 100 with respect to  $y$ . Here  $\Delta y = 0.05$ , and  $\Delta x = 0.0866$ .

The number of  $y$ -mesh points in the computing grid is made larger in order to obtain more precise values of the fundamental flow parameters ( $\rho$ ,  $\rho u$ ,  $\rho v$ ,  $e$ ) on both the conical and the cylindrical parts of the body.

The variation of the fundamental flow parameters on the conical and cylindrical parts of the body is checked continuously throughout the computing process, and the parameters are subsequently compared with tabulated values. On the conical surface and in the flow region next to it the numerical values are compared with the values tabulated in [7], in which the relative error of the solution of the difference equations is a few thousandths of a percent. On the cylindrical surface and in the adjacent flow the numerical values of the flow parameters are compared with the values tabulated in [8] according to the Prandtl—Meyer equations with allowance for turning of the flow through  $30^\circ$  at the corner. The flow parameters around the conical part of the body are taken as the initial parameters in calculating the tabulated values.

It is judged that the agreement between the numerical and tabulated values is good if the flow parameters in the given regions differ by less than 0.5%. When this condition is satisfied, the first stage is terminated.

To illustrate the behavior of the flow in the first stage Fig. 1b gives the field of isobars formed as a result of transition of the flow to a steady distribution. From the positions of the isobars we can estimate the location and waveform of the bow shock. The behavior of the isobars in the vicinities of the corner points in both the fore and the aft regions indicates the generation of oblique shocks at those points. It is important to note that the isobar field at the aft part of the body and in the wake in Fig. 1b is obtained by numerical computation of the flow parameters in the second stage and is then compared with the isobar field of the first stage, i. e., the pressure fields of the two stages are matched.

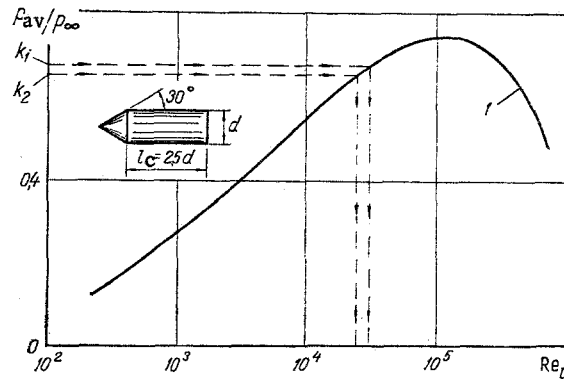


Fig. 3. Comparison of numerical and experimental data on the aft pressure versus Reynolds number. 1) From [2];  $K_1 = 0.68$ ,  $K_2 = 0.65$ .

In the second stage the same total number of mesh points is retained in the investigated region (6000), but the actual dimensions of the computing grid are altered somewhat; the number of  $y$ -mesh points is 20 (or 40), and the number of  $x$ -points is, respectively, 300 (or 150). Here  $\Delta y = (1/2)\Delta x = 0.05$  (or  $\Delta y = (1/2)\Delta x = 0.025$ ). This modification of the dimensions of the computing grid is motivated by the importance of analyzing in closer detail the behavior and certain characteristics of the flow precisely at the aft part of the body and in the zone immediately adjacent to it extending a length of five to ten base diameters.

During this stage of the computing process the variation of the flow parameters is again checked at the aft part of the body and at a certain point in the wake. It is judged that a stable steady-state solution is obtained if the flow parameters in the investigated regions vary less than 0.5% over the span of 50 mesh spacings.

Of practical interest in connection with the flow in the aft region is the behavior of the pressure along the radius of the aft section. An analysis of the numerical results on the aft pressure along the radius of the cylinder (see Fig. 2) shows that the local value of the aft pressure gradually decreases from the center of the cylinder toward its periphery. In the vicinity of the corner point a certain reduction is observed at first in the value of the aft pressure, but then, closer to the corner point, it increases very slightly (see curve 1 in Fig. 2). With a reduction in the spatial mesh spacing by one half the variation of the aft pressure along the radius of the cylinder is smoother (curve 2 in Fig. 2).

Using the local values of the aft pressure, we determine the area-average pressure  $P_{av}$  for both curves given in Fig. 2. For  $\Delta x = 0.1$  and  $\Delta y = 0.05$  the average pressure is 0.68. With  $P_{\infty} = 1$  the area-average aft pressure ratio is  $K_1 = P_{av}/P_{\infty} = 0.68$ . For  $\Delta x = 0.05$  and  $\Delta y = 0.025$  the ratio is  $K_2 = P_{av}/P_{\infty} = 0.65$ .

The average aft pressure ratios  $K_1$  and  $K_2$  thus obtained for both computing schemes are superimposed on the experimental curve  $P_{av}/P_{\infty} = f(Re)$  obtained by Kavanau [2] for a broad range of Reynolds numbers (see Fig. 3).

We note that the numerical results on the aft pressure and the experimental data of Kavanau refer to the same values of the parameters characterizing both the impinging supersonic flow (freestream  $M_{\infty} = 2.84$ ) and the geometry of the cone-cylinder configuration.

The comparison of the numerical results on the aft pressure with the experimental data leads to the conclusion that the numerical experiment on supersonic flow of an ideal gas in the wake of an axisymmetrical body is consistent in its main features with the true flow at Reynolds numbers of order  $(3 \text{ to } 3.5) \cdot 10^4$ .

This conclusion is supported by the behavior of the flow parameters in the wake of the body. Figure 4 gives profiles of the axial velocity component in the wake and the field of instantaneous velocities obtained in the second stage of computation. In this scheme  $\Delta x = 0.05$ ,  $\Delta y = 0.025$ , the distance from the aft section to the edge of the computing grid is  $S = 7$  base diameters, and the number of integration steps is  $n = 3000$ . It is evident from Fig. 4 that the flow is stable. The reverse-circulation zone spans a distance corresponding to two base diameters along the longitudinal axis. The upper boundary of this zone is near the line  $u = 0$  (Fig. 4a), and its lower boundary is before the symmetry axis (Fig. 4b).

The flow parameters are checked continuously at a point on the wake axis, at a distance of about one diameter from the aft section (point B in Fig. 4b). It is at this point that the minimum pressure is observed in

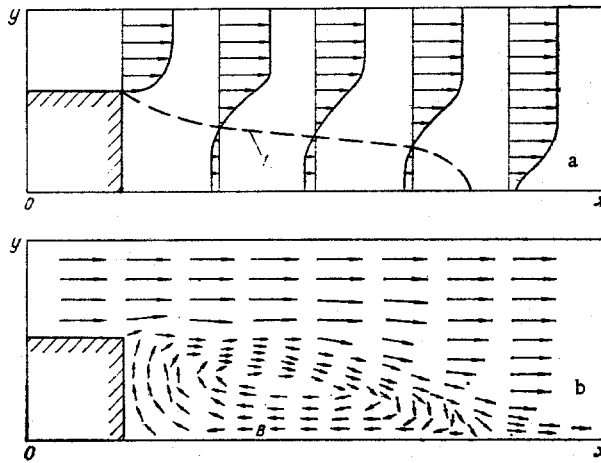


Fig. 4. Instantaneous velocity field in the wake. a) Profiles of axial velocity component (curve 1 represents  $u = 0$ ); b) total field pattern (B indicates the point at which the parameters are checked).

the reverse-circulation zone  $p_B = 0.61$ ), along with the maximum absolute value of the negative axial velocity component  $P_B = -0.6$ ).

In the other scheme, with  $\Delta x = 0.1$ ,  $\Delta y = 0.05$ ,  $S = 10$  diameters, and  $n = 3000$ , the pressure and axial velocity component at the check point B scarcely change ( $u_B = 0.63$ ;  $u_B = -0.58$ ). Neither do the dimensions of the wake change, even though in this scheme the dimensions of the computing grid are increased somewhat.

Thus, our numerical experiment on supersonic flow in the wake of an axisymmetrical body makes it possible to estimate the viscosity introduced by the maximally stable shock-smearing difference scheme [1] into the analyzed flow. The value of this "scheme" (artificial) viscosity corresponds to a physical viscosity characterized by Reynolds numbers  $(3 \text{ to } 3.5) \cdot 10^4$ .

#### NOTATION

$x$ , axial coordinate;  $y$ , radial coordinate;  $t$ , time;  $p$ , pressure;  $\rho$ , density;  $u$ , axial velocity component;  $v$ , radial velocity component;  $e$ , total specific energy;  $\rho(u^2 + v^2)/2 + p/(\gamma - 1)$ ;  $\gamma$ , specific heat ratio;  $\bar{a}$ , sound velocity;  $M$ , Mach number;  $Re$ , Reynolds number;  $\Delta x$ , mesh spacing of computing grid along  $x$ ;  $\Delta y$ , the same for  $y$ ;  $\Delta t$ , time spacing;  $k$ , axial index of computing mesh point,  $l$ , radial index of computing mesh point;  $p_\infty$ ,  $\rho_\infty$ ,  $M_\infty$ , freestream parameters;  $p_B$ ,  $\rho_B$ ,  $M_B$ , flow parameters at check point;  $r_c$ ,  $l_c$ , radius and length of cylindrical part of body;  $S$ , distance from aft section to edge of the computing grid;  $P_{av}$ , area-average pressure;  $K_1$ ,  $K_2$ , pressure coefficients.

#### LITERATURE CITED

1. V. B. Balakin and V. V. Bulanov, *Inzh.-Fiz. Zh.*, **27**, No. 3 (1974).
2. L. L. Kavanau, *J. Aeronaut. Sci.*, **21**, No. 4, 257-260 (1954).
3. V. I. Myshenkov, *Izv. Akad. Nauk SSSR, Mekh. Zhidk. Gaza*, No. 4, 10 (1972).
4. I. Yu. Brailovskaya, N. S. Kokoshinskaya, and L. V. Kuznetsova, in: *Numerical Methods of Continuum Mechanics [in Russian]*, Vol. 2, Novosibirsk (1971), p. 4.
5. O. M. Belotserkovskii and Yu. M. Davydov, in: *Selected Problems in Applied Mechanics [in Russian]*, Moscow (1974), p. 83.
6. P. Kutler and H. Lomax, in: *Numerical Methods in Fluid Mechanics [Russian translation]*, Mir, Moscow (1973), p. 126.
7. K. I. Babenko, G. P. Voskresenskii, A. N. Lyubimov, and V. V. Rusanov, *Three-Dimensional Ideal-Gas Flow past Smooth Bodies [in Russian]*, Nauka, Moscow (1964).
8. G. S. Roslyakov (editor), *Tables of Gasdynamic Functions [in Russian]*, VTs MGU, Moscow (1965).